Journal of Chromatography, 384 (1987) 91–103
Elsevier Science Publishers B.V., Amsterdam — Printed in The Netherlands

CHROMSYMP. 1021

PEAK-DECAY METHOD FOR THE MEASUREMENT OF DISSOCIATION RATE CONSTANTS BY HIGH-PERFORMANCE AFFINITY CHROMATOGRAPHY

ROBERT M. MOORE and RODNEY R. WALTERS*,*
Department of Chemistry, Iowa State University, Ames, IA 50011 (U.S.A.)

SUMMARY

A new method was described for the measurement of dissociation rate constants of biological complexes by affinity chromatography. Theory and computer modeling were used to establish conditions such that each solute molecule would undergo only a single dissociation step during its passage through the column. As a result, the dissociation rate constant could easily be determined from the slope of the logarithm of the tailing portion of the peak. An experimental system, consisting of immobilized concanavalin A and a fluorescent sugar, was used to test the theory and to compare the peak-decay method with the conventional isocratic method.

INTRODUCTION

Affinity chromatography can be used to estimate the association and dissociation rate constants of biological complexes. Several experimental modes may be used for such measurements.

The broadening of a band of solute, applied to a column containing immobilized affinity ligand, is measured in the isocratic, competitive elution, zonal mode by using one or more competing inhibitor concentrations[1,2]. Although this method has been applied several times, the measured rate constants have generally been one or more orders of magnitude lower than expected from free solution studies[3–6]. A recent paper has suggested that these apparent low values may have been due to inadequacies in the band-broadening theories used for the calculations and/or the dominance of mass transport-caused band-broadening over slow adsorption–desorption kinetic band-broadening[7].

Rate and equilibrium constants may also be measured in the frontal mode by utilizing the shapes and positions of the break-through curves for several concentrations of solute applied to the column[8]. This method has not yet been examined with biological complexes having known rate constants.

In the split-peak zonal mode, the association rate constant can be determined

* Present address: Drug Metabolism Research, The Upjohn Company, Kalamazoo, MI 49001, U.S.A.

0021-9673/87/$03.50

using data from several flow-rates under conditions where some of the solute does not have time to become adsorbed on immobilized ligand during its passage through the column and is thus eluted in the column void volume[9]. This method has also not yet been tested with complexes of known rate constants.

This paper describes a new method for determining dissociation rate constants. This method, called the "peak-decay" method, eliminates certain disadvantages of the isocratic method; specifically, the need to measure peak variances, the need to perform calculations as a function of capacity factor (k'), and the need to use linear elution conditions. The peak-decay method does require the use of a competitive inhibitor; however, the kinetic effects of non-competitive eluents can also be studied.

THEORY

The theory for the peak-decay method is based on the model utilized by Hethcote and DeLisi[1] for isocratic affinity chromatography. The model assumes that there are two reversible rate processes occurring in the column, a diffusional mass transport step and an adsorption–desorption step:

$$E_e \underset{k_{-1}}{\overset{k_1}{\rightleftharpoons}} E_p \tag{1}$$

$$E_p + L \underset{k_{-3}}{\overset{k_3}{\rightleftharpoons}} E_p\text{–}L \tag{2}$$

The symbol E represents the solute applied to the column and present in the flowing mobile phase (or excluded volume, e), stagnant mobile phase (or pore volume, p), or bound to immobilized ligand (L). The diffusional rate constants (k_1, k_{-1}) are related to the excluded volume and pore volume accessible to the solute[1]:

$$\frac{k_1}{k_{-1}} = \frac{V_p}{V_e} \tag{3}$$

The adsorption and desorption rate constants (k_3, k_{-3}) are related to K_3, the equilibrium binding constant[3]:

$$\frac{k_3}{k_{-3}} = K_3 \tag{4}$$

In an isocratic experiment, a competing inhibitor (I) is usually present in the mobile phase to control retention. If the inhibitor binds to L rather than to E, *i.e.*, reversed-role affinity chromatography[2], then the band-broadening due to the two kinetic processes is given by[7]

$$H_{sm} = \frac{2uV_p(1 + V_m k'/V_p)^2}{V_m k_{-1}(1 + k')^2} \tag{5}$$

$$H_k = \frac{2\,uk'}{k_{-3}(1 + k')^2} \tag{6}$$

where H_{sm} is the plate height due to slow mass transfer between the moving and stagnant mobile phase, H_k is the plate height due to slow adsorption–desorption kinetics, u is the linear velocity of the mobile phase, and V_m is the void volume ($V_p + V_e$). We have previously shown[7] that these equations are identical in form to the well known equations derived by Horváth and Lin[10]. However, the equations above do not include interparticle band-broadening processes, such as eddy diffusion.

Consider a modification of the isocratic experiment in which the adsorption sites are first saturated with solute (by means of frontal rather than zonal application of E), then the column is washed to remove excess E. A high concentration of competing inhibitor is next applied to the column in a frontal mode so that retention of E is suddenly reduced nearly to zero. The solute is then eluted under isocratic conditions. Since the inhibitor does not itself cause dissociation of the E–L complex, but instead functions to prevent readsorption by filling any empty adsorption sites, the value of k_{-3} is not altered.

The elution profile of the solute leaving the column cannot, in general, be easily used to extract kinetic data. However, if extreme conditions are utilized, useful information may be obtained. In particular, if readsorption and diffusion back into stagnant mobile phase are prevented, then only a single dissociation will take place for each solute–ligand complex. Then the peak profile should resemble an exponential decay with rate constant k_{-1} or k_{-3}, whichever is smaller.

Mathematically, the peak-decay method is described by the reactions

$$E_p\text{–}L \xrightarrow{k_{-3}} E_p + L \tag{7}$$

$$E_p \xrightarrow{k_{-1}} E_e \tag{8}$$

which are just the irreversible equivalents of equilibria 1 and 2. To prevent reversibility completely requires infinitely large competing inhibitor concentrations (so that $k' = 0$) and a column length of zero (so that diffusion back into the stagnant mobile phase is prevented). Under such conditions, the differential equations describing reactions 7 and 8 are as follows:

$$\frac{dm_{E_p\text{–}L}}{dt} = -k_{-3}m_{E_p\text{–}L} \tag{9}$$

$$\frac{dm_{E_p}}{dt} = k_{-3}m_{E_p\text{–}L} - k_{-1}m_{E_p} \tag{10}$$

where m is the number of moles of solute. Assuming that all of the solute is initially adsorbed and of total amount m_{E_0}, and that $k_{-3} < k_{-1}$, the equations can be solved[11] in terms of the amount eluted up to time t:

$$m_{E_e} = \frac{m_{E_0}}{k_{-1} - k_{-3}} \{k_{-1}[1 - \exp(-k_{-3}t)] - k_{-3}[1 - \exp(-k_{-1}t)]\} \quad (11)$$

The elution profile is the derivative of eqn. 11:

$$\frac{dm_{E_e}}{dt} = \frac{k_{-1}k_{-3}m_{E_0}}{k_{-1} - k_{-3}} [\exp(-k_{-3}t) - \exp(-k_{-1}t)] \quad (12)$$

If $k_{-3} \ll k_{-1}$, then eqn. 12 reduces to a simple exponential decay. The rate constant k_{-3} is obtained from the slope of a plot of the natural logarithm of the elution profile:

$$\ln \frac{dm_{E_e}}{dt} = \ln(m_{E_0}k_{-3}) - k_{-3}t \quad (13)$$

An analogous derivation can be made for the case where $k_{-1} < k_{-3}$.

The use of a finite inhibitor concentration and column length will result in some readsorption of solute onto the stationary phase and some diffusion of solute back into the stagnant mobile phase. This will cause further band-broadening, a shallower elution profile, and an apparent low value for the rate constant determined from the slope of the logarithm of the profile. However, it is possible to find useful conditions under which eqn. 13 provides a reasonably accurate description of the elution profile. These conditions are most easily obtained by means of computer simulations.

The computer model used here is based on the first-order reactions equivalent to reactions 1 and 2:

$$E_e \underset{k_{-1}}{\overset{k_1}{\rightleftharpoons}} E_p \underset{k_{-3}}{\overset{k_3^*}{\rightleftharpoons}} E_p\text{–}L \quad (14)$$

The first-order adsorption rate constant, k_3^*, is equal to $k_3 m_L/V_p$, where m_L is the number of moles of ligand in the column. The general solution to this reaction was derived by Rakowski[12] and can be easily recast in terms of k', V_p, and V_e.

To utilize reaction 14 for column chromatography, the convective mass transport of E in the excluded volume must also be taken into account. This can be done by dividing an imaginary column longitudinally into a large number of slices and radially into three regions (flowing and stagnant mobile phase, and stationary phase). Each iteration of the computer consists of equilibrating the solute between the three radial regions according to the solution of reaction 14, then moving the solute in the excluded volume of one slice into the excluded volume of the next slice (the excluded linear velocity, u_e, is one slice per iteration). The solute leaving the last slice is monitored.

The time between recalculation of the amounts of solute in each slice and phase is one iteration. If the rate constants are approximately one iteration^{-1} or larger, then the system is close to equilibrium and the elution profile can be predicted from the Craig distribution[13]. This undesirable characteristic can be avoided by using smaller values for the rate constants ($\lesssim 0.1$ iteration^{-1}). By decreasing the rate

constants and proportionally increasing the number of slices of column length, one can easily ensure that the results have converged to a single value. This model was previously used for isocratic studies and it was shown that the band-broadening obtained was identical to that predicted by eqns. 5 and 6[7].

For use in the peak-decay mode, the program is modified so that solute is initially distributed throughout the column. At time zero, a plug of mobile phase containing inhibitor begins to move down the column, k' decreases to some predetermined value behind the mobile-phase front, and the solute begins to undergo dissociation, readsorption, and diffusion, just as in the isocratic method.

The simulation does not take into account broadening and dilution of the competing inhibitor front, nor does it take into account the finite number of ligand sites. Inclusion of the former process in the model would probably cause the elution profile to be broader, while the latter would cause it to be narrower.

EXPERIMENTAL

Reagents

Concanavalin A (Con A), type IV, 4-methylumbelliferyl α-D-mannopyranoside (MUM), and 4-methylumbelliferyl α-D-galactopyranoside (MUGA) were purchased from Sigma (St. Louis, MO, U.S.A.). The Hypersil WP-300, 5-μm particle diameter, was purchased from Alltech (Deerfield, IL, U.S.A.). Mannose and 1,1′-carbonyldiimidazole were from Aldrich (Milwaukee, WI, U.S.A.).

Apparatus

A Model 334 liquid chromatograph (Beckman, Berkeley, CA, U.S.A.) was modified by replacing the mixing chamber with a tee. A Model 757 UV–VIS detector (Kratos, Ramsey, NJ, U.S.A.) with a 12-μl flowcell was used for detection at 316 nm. An Apple IIe computer (Cupertino, CA, U.S.A.) with an Interactive Microware interface (State College, PA, U.S.A.) was used for data acquisition. A refrigerated circulating bath (Fisher, Chicago, IL, U.S.A.) was used to maintain the temperature of the column.

Computer simulations were performed on a National Advanced Systems 9160 computer (Mountain View, CA, U.S.A.).

Procedure

Diol-bonded Hypersil WP-300 was prepared according to a published procedure[14]. A 2-ml volume of a solution containing 9.8 mg/ml purified[15] Con A in 0.50 *M* sodium acetate buffer (pH 5.00), containing 1.0 m*M* calcium chloride and 1.0 m*M* manganese chloride, was immobilized at 4°C for seven days using the 1,1′-carbonyldiimidazole procedure[16,17] and 0.1 g diol-bonded silica. The immobilized Con A concentration was found to be 38 mg/g silica on the basis of the bicinchoninic protein assay (Pierce, Rockford, IL, U.S.A.). The silica was packed into a 6.3 mm × 2.1 mm I.D. column of published design[18] using the vacuum slurry packing method[19].

The weak mobile phase used for chromatographic experiments was the buffer described above. The strong mobile phase contained, in addition, 0.1 *M* mannose.

In a typical experiment, the column was first equilibrated with weak mobile phase at 1 ml/min and 25°C. A 2.4-ml injection of $1 \cdot 10^{-5}$ *M* MUM in weak mobile

phase was then made, and the excess MUM was removed by washing the column for 3.5 min. A step change to a flow-rate of 10 ml/min and the strong mobile phase was then made, and MUM elution data were acquired for 15 s at a rate of 10 points per second.

The slope of the natural logarithms of the tailing portion of the peak was calculated using the method of Guggenheim[20]. Baseline correction using a blank run was found to be unnecessary because the baseline disturbance due to the mobile phase change did not overlap with the tail of the MUM peak.

RESULTS AND DISCUSSION

Computer simulations

Fig. 1 shows two peak-decay profiles, calculated from eqn. 12 by using different values of k_{-1}/k_{-3}. Note that when k_{-1} and k_{-3} were similar in magnitude, the peak was broader and the logarithm of the profile was somewhat curved, as expected from the theoretical equation. In such a situation, an arbitrary choice of the portion of the profile to use in determining the slope had to be made. All of the slopes from computer simulations were measured in the following way: the times corresponding to the top of the peak profile and the point where 99% of the solute was eluted were determined. The time between these points was divided into five equal segments. The slope of the second segment (from the peak) was determined by linear least squares fitting of the points. The segment used is marked in Fig. 1. This particular segment was chosen because it most closely duplicated the region used in the experimental data.

Plots identical to Fig. 1 were obtained from the two-step reversible computer model when the column length and k' were both very small. This observation plus the previous isocratic experiments[7] support the accuracy of the computer model with respect to the mathematical model of Hethcote and DeLisi[1,2].

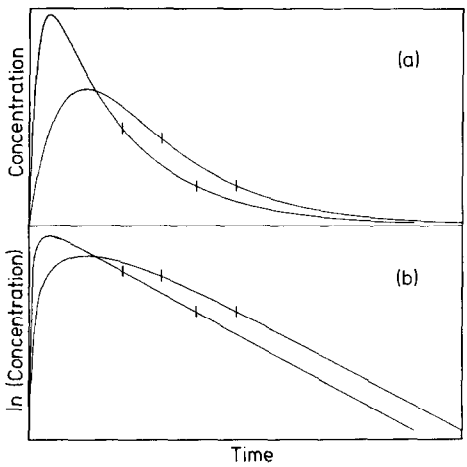

Fig. 1. Peak-decay profiles (a) and the natural logarithm of the profiles (b) calculated from eqn. 12 for the conditions $k_{-1}/k_{-3} = 10$ (taller peak) and $k_{-1}/k_{-3} = 2$ (shorter peak). The vertical marks indicate the region used for slope measurements.

The computer model was first used to examine the case in which retention was large enough that significant readsorption could occur but the column length was still insignificantly small. Rate constants were measured from simulated peak-decay profiles as a function of k' and k_{-1}/k_{-3} (Fig. 2). The slopes of the logarithm plots were normalized by dividing by the smaller of k_{-1} or k_{-3}. Thus, a normalized slope of 1.0 indicated that the rate constant of the slowest step could be accurately measured. Note that the slopes were always low when k_{-1} was similar in magnitude to k_{-3}. However, if k_{-1} was at least 10-fold larger or smaller than k_{-3}, then the smaller of the two rate constants could be measured with good accuracy when k' was small.

Fig. 2 also shows that the accuracy of the apparent rate constants declined as k' increased. This is because multiple adsorption and desorption steps began to take place and caused additional band-broadening. Interestingly, at high k', the plot was very asymmetric and indicated that when $k_{-1}/k_{-3} > 100$, k_{-3} could still be determined accurately, but when $k_{-1}/k_{-3} < 0.01$, k_{-1} could not be determined accurately. This difference was due to the fact that in the former case, as soon as the adsorbed complex dissociated, the solute immediately diffused out of the pore and was washed from the column. In the latter case, adsorbed solute and free solute in the pore volume were essentially in equilibrium, and so the solute diffused out of the pore more slowly than if all the solute were free.

Plots drawn with different values of V_p/V_e were similar to Fig. 2 but shifted vertically. Examination of the data indicated that plotting the data as a function of $k'V_m/V_p$ caused the data generated at different V_p/V_e values to merge into a single family of curves. From such a plot it was possible to determine the maximum allowable value of $k'V_m/V_p$ such that k_{-1} or k_{-3} could be determined accurately.

As the column length increased to significant values (Fig. 3), there was a greater likelihood of multiple adsorption–desorption steps with the result that the elution profiles became less steep. This was not really a function of the column length itself,

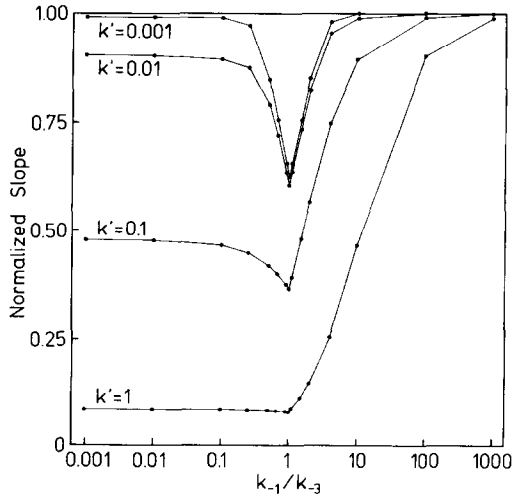

Fig. 2. Plot of normalized slope from computer simulations of peak-decay profiles as a function of k_{-1}/k_{-3} and k' for $V_p/V_e = 0.1$ and zero column length.

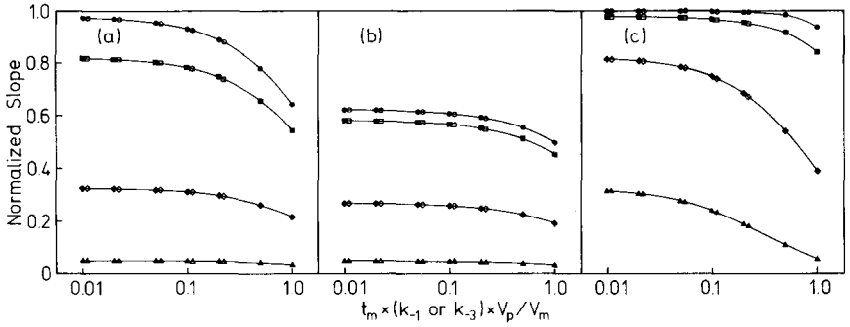

Fig. 3. Plots of normalized slope from computer simulations of peak-decay profiles as a function of void time for $k_{-1}/k_{-3} = 0.1$ (a), 1.0 (b), and 10.0 (c). From top to bottom, the curves represent 10-fold increases in $k'V_m/V_p$ beginning at a value of 0.02 for $V_m/V_p = 2$ (solid symbols) and $V_m/V_p = 10$ (open symbols).

but rather of the residence time of solute in the column (*i.e.* the void time, t_m) relative to the rate constants. The factor V_m/V_p also was important here; hence, the normalized slope is plotted in Fig. 3 *vs.* the product of t_m, V_p/V_m, and the smaller of k_{-1} or k_{-3}. From this plot, the maximum allowable void time could be determined.

By examination of the data used to prepare Figs. 2 and 3, conditions were found such that the smaller of k_{-1} or k_{-3} could be measured with less than a 5% error. The conditions for accurate determination of k_{-1} were:

$$k_{-1}/k_{-3} \leq 0.1 \tag{15}$$
$$t_m k_{-1} V_p/V_m \leq 0.05 \tag{16}$$
$$k'V_m/V_p \leq 0.02 \tag{17}$$

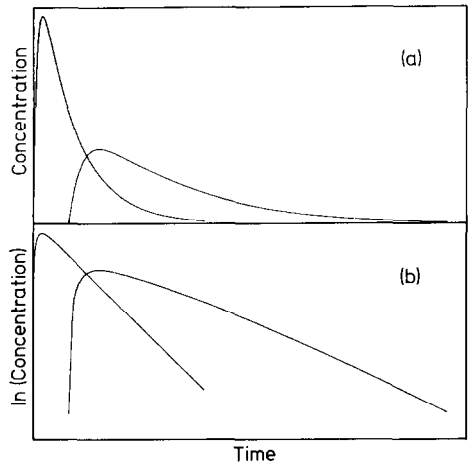

Fig. 4. Computer-simulated peak-decay profiles (a) and the natural logarithms of the profiles (b) for $k_{-1}/k_{-3} = 10$ and $V_p/V_e = 1$. For the taller peak, $t_m k_{-3} V_p/V_m = 0.01$ and $k'V_m/V_p = 0.02$. For the shorter peak, the quantities are 1.0 and 2.0, respectively.

The conditions for accurate determination of k_{-3} were:

$$k_{-1}/k_{-3} \geq 10 \quad (18)$$
$$t_m k_{-3} V_p/V_m \leq 0.2 \quad (19)$$
$$k' V_m/V_p \leq 0.2 \quad (20)$$

Other conditions may also be acceptable. For example, if $k_{-1}/k_{-3} \geq 100$, then Fig. 2 shows that the requirement for k' could be relaxed somewhat.

Fig. 4 shows two peak profiles generated from the computer model. One was a nearly ideal case in which $k_{-1}/k_{-3} = 1.0$, $V_p/V_e = 1$, $t_m k_{-3} = 0.02$, and $k' = 0.01$. The normalized slope was 0.998, *i.e.* only 0.2% less than the expected value. The other curve was for a case where $t_m k_{-3} = 2$ and $k' = 1$. The normalized slope decreased to 0.386 and thus the apparent rate constant was significantly less than the expected value.

Effect of heterogeneity

If there were heterogeneity in the values of k_{-1} or k_{-3}, then eqn. 12 could be expanded to include more terms, each with its own m_{E_0}, k_{-1}, and k_{-3}. The logarithm plots would then be the sum of several exponential terms, leading to a plot which flattens as time increased (just the opposite of Fig. 1b, where the plot became steeper with time).

If the slope were measured late in the tail of the peak, it always approached the smallest of the individual rate constants because the faster-decaying solute molecules had already left the column. If the slope were measured as described earlier, the apparent rate constant turned out to be quite close to the apparent value that would have been obtained from an isocratic experiment, *i.e.* weighted toward the smallest rate constant.

Comparison with isocratic methods

Since both the peak-decay and isocratic methods utilize competing inhibitors, it is useful to compare the potential advantages of one method over the other.

In the isocratic method, one must generally correct the total plate height for the contributions due to H_{sm} and the eddy diffusion/mobile-phase mass transfer plate height. This involves mesurement of u, V_p, V_e, and k_{-1} and recalculation of the plate heights as a function of k', all of which introduce significant uncertainty in the final results[7]. In contrast, the rate constant is obtained directly from the slope of the logarithm of the detector response in the peak-decay method.

Some of the calculation problems of the isocratic method can be avoided if the entire measured plate height is attributed to H_k. Then only u and k' need to be measured (eqn. 6). Consider the case where $k_{-1}/k_{-3} = 10$ and $V_p/V_e = 1$. Since at $k' = 10$, $H_{sm}/H_k = 2.2$ from eqns. 5 and 6, the apparent value of k_{-3} would be only 31% of its true value if H_{sm} were not subtracted from the total plate height. A more favorable case is at $k' = 1$, since H_k reaches a maximum at that point but H_{sm} has not increased to its maximum value. The apparent rate constant would still be only 69% of its true value at this point. In contrast, for the same system but with k' and t_m adjusted in accordance with eqns. 19 and 20, the apparent value of k_{-3} would be at least 95% of its true value. Thus, with the peak-decay method, one can measure

k_{-3} accurately when $k_{-1}/k_{-3} \geq 10$. With the isocratic method, similar accuracy requires $k_{-1}/k_{-3} \geq 100$.

Other practical advantages of the peak-decay method over the isocratic method include (a) better precision, since slopes rather than variances of the peak profiles are measured, (b) shorter analysis times, since dissociation only needs to take place once rather than many times, (c) reasonable analysis times, even in cases where k_{-3} is quite small, and (d) improved detectability, because the column can be saturated with solute.

Potentially offsetting these advantages are the need to use very high inhibitor concentrations to reduce k', and high flow-rates or short columns to minimize t_m in cases where k_{-3} is moderately large. Since there is a step change in mobile phase at time zero, detectability may also be adversely affected by refractive-index effects.

Preliminary calculations taking into account analysis time, inhibitor concentration, flow-rate, column size, and detectability are described in ref. 21 and may be useful in determining whether isocratic or peak-decay experiments are feasible in particular situations.

Experimental data

A system consisting of an immobilized protein, Con A, as the ligand, and the sugars MUM and mannose as solute and inhibitor, respectively, were utilized for the experimental studies. From previous isocratic measurements, approximate values of the rate constants were known: $k_{-1} \approx 120\ s^{-1}$; $k_{-3} \approx 2\ s^{-1}$ (ref. 7). The ratio of the rate constants easily met the criterion of eqn. 18. For the Hypersil column used, $V_p/V_m \approx 0.44$. Thus, eqn. 19 required $t_m \leq 0.23$ s. This was a severe requirement, and therefore high flow-rates and/or small columns were needed to measure a dissociation rate this fast. A 6.3 mm × 2.1 mm I.D. column was chosen. With a void volume of approximately 14 μl, the flow-rate needed was 3.7 ml/min. To meet the criterion of eqn. 20 required $k' \leq 0.088$. From isocratic studies, the binding constants for the sugars were determined: K_3 (MUM) = 45 000 M^{-1}; K_2 (mannose) = 1500 M^{-1}. From break-through curve and protein assay data, the number of moles of active Con A in the column was estimated to be 18 nmol. From eqn. 3 of ref. 7, the minimum inhibitor concentration was calculated to be 0.44 M.

Fig. 5 shows the data from a typical experimental run at a flow-rate of 10 ml/min and 0.1 M mannose concentration. The logarithmic plots (Fig. 5b) typically were somewhat concave, but the slope could be determined with excellent precision [±3% relative standard deviation (R.S.D.) from the slope of a single run, ±5% R.S.D. for replicate runs]. As pointed out earlier, one possible cause of the concave plot could be heterogeneity in the immobilized Con A.

Experiments were performed at several flow-rates (Fig. 6) and mannose concentrations (Fig. 7) to determine whether the data obeyed eqns. 19 and 20. Both experiments exhibited the expected trends, with the apparent rate constants reaching a plateau value of approximately 1.78 s^{-1} at high flow-rate (small t_m) and high inhibitor concentration (small k').

The flow-rate and inhibitor concentration needed to reach the plateau value of k_{-3} were somewhat different than those predicted above. To examine this further, the experimental system was modeled with the parameters listed above and a value of 1.82 s^{-1} for k_{-3}. The simulated data are also shown in Figs. 6 and 7. From Fig.

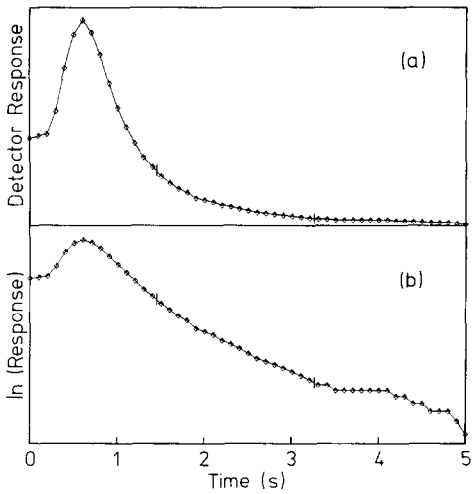

Fig. 5. An experimental peak-decay profile (a) and natural logarithm of the profile (b) for MUM eluted from an immobilized Con A column at a flow-rate of 10 ml/min with a mannose concentration of 0.1 *M*. The vertical marks indicate the region used for slope measurements.

6, it is apparent that the model predicted only a small change in the apparent rate constants over the flow-rate range used, whereas the actual change was much greater. The difference was probably caused by factors not taken into account in the model, such as dispersion of the inhibitor front as it passed through the column, or eddy diffusion/mobile-phase mass-transfer effects on the solute band-broadening. On the other hand, Fig. 7 shows better agreement between experimental and predicted values of k_{-3} as a function of inhibitor concentration. Some of the discrepancies between theory and experiment in both Figs. 6 and 7 could be due to inaccuracies in the values of m_L, V_m, etc. used in the simulations.

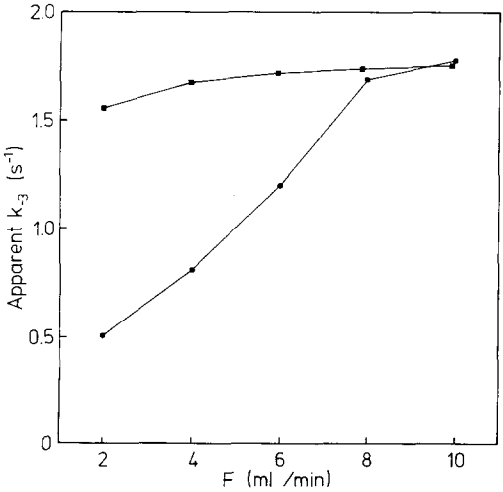

Fig. 6. Experimental (●) and theoretical (■) plots of the apparent value of k_{-3} *vs.* flow-rate for the Con A–sugar system with 0.1 *M* mannose as inhibitor.

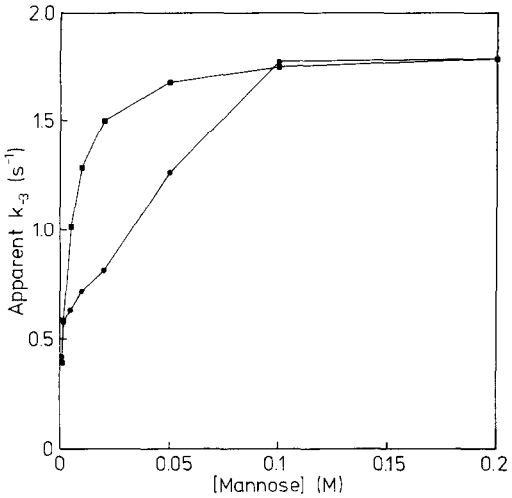

Fig. 7. Experimental (●) and theoretical (■) plots of the apparent value of k_{-3} *vs.* inhibitor concentration for the Con A–sugar system at a flow-rate of 10 ml/min.

Another factor examined was the effect of washing the column with buffer to remove excess MUM prior to the step change in mobile phase. The calculated k' for MUM in the absence of inhibitor was 58. It is apparent that with the small void volume of the column, all the MUM would be eluted isocratically in a relatively short time period. To examine this, the length of the wash time was varied from 2 to 5 min at 1 ml/min. The rate constants were measured using a flow-rate of 10 ml/min and 0.1 *M* mannose. Table I shows the results of this study. No change in the rate constant was observed at wash times of less than 4 min. The apparent change at longer wash times may have been due to experimental error in the data, as the amount of MUM remaining in the column declined.

Taking into account column-to-column reproducibility, the dissociation rate constant for the MUM–immobilized Con A complex was 1.8 ± 0.1 s^{-1} at 25°C. This is in excellent agreement with a value of 2.0 ± 0.6 s^{-1} from the best of our previous isocratic studies[7] and in fair agreement with a value of 3.4 s^{-1} from free solution studies[22]. Since the equilibrium binding constant appears to be larger for

TABLE I

EFFECT OF COLUMN WASHING PRIOR TO ELUTION OF MUM

Wash time (min)	*Apparent* k_{-3} (s^{-1})	*Relative peak area*
2.0	1.54	1.00
2.5	1.79	0.40
3.0	1.77	0.31
3.5	1.75	0.21
4.0	1.76	0.13
4.5	1.10	0.09
5.0	1.18	0.06

immobilized Con A[7], the values of k_3 calculated from eqn. 4 for immobilized Con A ($8.1 \cdot 10^4\ M^{-1}\ s^{-1}$) and free Con A ($11.2 \cdot 10^4\ M^{-1}\ s^{-1}$) are in good agreement. Further work is underway to determine the effect of temperature on the rate and equilibrium constants.

CONCLUSIONS

Since there were some discrepancies between the model used to obtain eqns. 15–20 and the experimental data from the Con A–sugar system, particularly in the case of flow-rate effects, it is suggested that eqns. 15–20 be used only to establish initial conditions for peak-decay measurements. Flow-rate and inhibitor concentration studies should be performed to ensure that the "plateau" value of the dissociation rate has been reached.

The superior precision of the rate constants obtained from peak-decay measurements compared to isocratic measurements suggest that the peak-decay method should be the method of choice for affinity chromatographic estimation of dissociation rate constants. The method should be useful for rate constants of monovalent interactions ranging from about 10 s^{-1} to less than $10^{-3}\ s^{-1}$.

ACKNOWLEDGEMENT

This work was supported by the National Science Foundation under Grant CHE-8305057.

REFERENCES

1 H. W. Hethcote and C. DeLisi, *J. Chromatogr.*, 248 (1982) 183.
2 H. W. Hethcote and C. DeLisi, in I. M. Chaiken, M. Wilchek and I. Parikh (Editors), *Affinity Chromatography and Biological Recognition*, Academic Press, New York, 1983, p. 119.
3 I. M. Chaiken, *Anal. Biochem.*, 97 (1979) 1.
4 V. Kasche, K. Buchholz and B. Galunsky, *J. Chromatogr.*, 216 (1981) 169.
5 K. Nilsson and P.-O. Larsson, *Anal. Biochem.*, 134 (1983) 60.
6 A. J. Muller and P. W. Carr, *J. Chromatogr.*, 284 (1984) 33.
7 D. J. Anderson and R. R. Walters, *J. Chromatogr.*, 376 (1986) 69.
8 H. A. Chase, *J. Chromatogr.*, 297 (1984) 179.
9 D. S. Hage, R. R. Walters and H. W. Hethcote, *Anal. Chem.*, 58 (1986) 274.
10 C. Horváth and H.-J. Lin, *J. Chromatogr.*, 149 (1978) 43.
11 J. H. Espenson, *Chemical Kinetics and Reaction Mechanisms*, McGraw-Hill, New York, 1981, p. 65.
12 A. Rakowski, *Z. Phys. Chem.*, 57 (1906) 321.
13 B. L. Karger, L. R. Snyder and C. Horvath, *An Introduction to Separation Science*, Wiley, New York, 1973, p. 110.
14 R. R. Walters, in P. D. G. Dean, W. S. Johnson and F. A. Middle (Editors), *Affinity Chromatography: A Practical Approach*, IRL Press, Oxford, 1985, p. 25.
15 B. A. Cunningham, J. L. Wang, M. N. Pflumm and G. M. Edelman, *Biochemistry*, 11 (1972) 3233.
16 G. S. Bethell, J. S. Ayers, W. S. Hancock and M. T. W. Hearn, *J. Biol. Chem.*, 254 (1979) 2572.
17 S. C. Crowley, K. C. Chan and R. R. Walters, *J. Chromatogr.*, 359 (1986) 359.
18 R. R. Walters, *Anal. Chem.*, 55 (1983) 591.
19 R. M. Moore and R. R. Walters, *J. Chromatogr.*, 317 (1984) 119.
20 E. A. Guggenheim, *Philos. Mag.*, 2 (1926) 538.
21 R. R. Walters, in I. M. Chaiken (Editor), *Analytical Affinity Chromatography*, CRC Uniscience, Boca Raton, in press.
22 R. M. Clegg, F. G. Loontiens, A. Van Landschoot and T. M. Jovin, *Biochemistry*, 20 (1981) 4687.